Robust Dynamic Tracking Control of a Modal Parameter Varying Spacecraft avoiding Vibration

Samsul Arefin, Didier Dumur, Aurelien Hot, Alain Bettachioli, Sihem Tebbani, Jean-Marie Pasquet

Robust Dynamic Tracking Control of a Modal Parameter Varying Spacecraft avoiding Vibration

Samsul Arefin
Université Paris-Saclay, CNRS, CentraleSupélec, *Laboratoire des signaux et systèmes*, CNES, *Structures and Mechanics Department,* Thales Alenia Space, *Competence Center Plateform & Integration France*
Cannes, France
samsul.arefin@centralesupelec.fr

Didier Dumur
Université Paris-Saclay, CNRS, CentraleSupélec, *Laboratoire des signaux et systèmes*,
91190, Gif sur Yvette, France
didier.dumur@centralesupelec.fr

Aurélien Hot
CNES, *Structures and Mechanics Department*
Toulouse, France
aurelien.hot@cnes.fr

Alain Bettachioli
Competence Center Plateform & Integration France
Thales Alenia Space
Cannes, France
alain.bettacchioli@testingsimulation.com

Sihem Tebbani
Université Paris-Saclay, CNRS, CentraleSupélec, *Laboratoire des signaux et systèmes*,
91190, Gif sur Yvette, France
sihem.tebbani@centralesupelec.fr

Jean-Marie Pasquet
Competence Center Plateform & Integration France
Thales Alenia Space
Cannes, France
jean-marie.pasquet@thalesaleniaspace.com

2021 9th International Conference on Systems and Control (ICSC) | 978-1-6654-0782-3/21/$31.00 ©2021 IEEE | DOI: 10.1109/ICSC50472.2021.9666719

***Abstract*—The vibration testing system of a large structure spacecraft presents inaccurate precision tracking and high oscillations in the neighborhood of its vibrational modes, particularly at higher frequencies. In the presence of varying modal parameters of a spacecraft such as the mode frequency and corresponding damping ratio, the performance of the controlled system degrades. Robust high precision tracking control of such systems with varying modal parameters is rarely addressed in the literature. A new closed-loop system architecture is proposed in this paper, based on a feedforward-feedback tracking control strategy involving an H_∞ controller. Simulation results show that the new architecture allows precise tracking of a sine sweep acceleration reference signal avoiding vibrations when sweeping through modes. Furthermore, it appears to be highly robust against varying parameters, model uncertainties, as well as the presence of sensor noise. The proposed controller also limits the control effort to avoid the actuator saturation. A minimal order controller is derived which makes it tractable for further industrial implementation.**

Keywords—Sine Sweep Tracking, Robust Vibration Control, Lightly Damped Spacecraft, Dynamic Tracking Error

I. INTRODUCTION

Vibration testing system is an essential part of the mechanical qualification of large space structures, as it has to survive severe vibratory conditions at the very beginning phase of the rocket launch [1]. Traditionally, in the coupled load analysis (CLA), the combined dynamical model of the spacecraft and the launcher are used to verify the absence of any coupling of vibrational modes between these two structures. This analysis requires a precise model of the spacecraft [1], which is identified through the vibration testing system. Current control architecture of the vibration testing system presents overshoot, high oscillations while the reference signal sweeps through the spacecraft's lightly damped mode frequencies [2][4][8]. This current strategy is based on a first-order sliding mode control [5], inducing the famous "chattering" phenomena, which is basically the non-smoothness of the command associated to the nonlinearities of the control law [6][7]. In this paper, the development of control strategies is considered to improve the tracking performance of the current vibration analysis system, while reducing the time of the vibration testing procedure by ensuring stability and robustness features.

In the literature of active vibration control, classical root locus-based controls are widely used [10] [11], which need a profound knowledge of control systems engineering, but also lack robustness against any modal parameter variation because of the pole-zero flip-flop phenomena [10][11]. On the other hand, there are some studies demonstrating very promising performances of active vibration control while using LQ, LQG, H_∞ control laws [3][11][12]. Although the studied systems show quite good performance, most of the studied cases are regulation problems [11][12]. In the study case, the frequency of the reference varies continuously and the system always remains in a transient state, never reaching a steady-state behavior [4]. We are therefore dealing with dynamic tracking error.

In [2], a mixed sensitivity based H_∞ control has been studied on a single vibrational mode system. The study shows a high level of tracking performance [2] as well as being robust against the variation of damping ratio and time delay, although it does not assess the case with varying mode frequencies [2]. Generally, the main drawback of the classical mixed sensitivity based H_∞ control is the pole-zero cancellation phenomenon of active vibration control problems [3][12][13] [14]. This phenomenon becomes critical when the system like spacecraft has very lightly damped modes [12]. In addition, the simplified second degree system does not include any anti-resonance, unlike a real satellite-vibrator model [2][12]. A μ synthesis-based control can be found in [12] to

address the active vibration control of a regulation problem, which shows better robustness against parameter variation of the plant compared to H_∞ synthesis. Despite, the μ-synthesis requires significant amount of synthesis time for a real complex dynamical system, also results in higher order controllers [15]. The complexity of μ controller makes it quite challenging to implement in a real-time context with a very high sampling rate framework [12].

In this paper, the proposed closed-loop architecture uses an H_∞ based multivariable feedback control with a feedforward action. The motivation of the research is to increase the bandwidth of the controller to tackle any errors in the closed loop. Therefore, the feedforward controller is used for faster response of reference tracking [22] and the 2 degree of freedom feedback controller is well known in the literature [23] for providing better tracking error and robustness properties than those of a single input-output controller.

The paper is structured as follows: Section II presents the spacecraft modeling issues. Section III introduces a systematic design procedure of the feedforward and feedback controller. Lastly, in Section IV, an analysis through different simulations illustrates the performance of the proposed control structure compared to the current nonlinear control.

II. Spacecraft Dynamical Model

In this section, the identified plant model of the spacecraft-interface will be simplified for the optimal order controller design. Secondly, the modal parameters of the plant have to be identified for the systems performance assessment.

A. Dynamical model

Fig. 1 illustrates the closed-loop architecture of the current vibration testing system. The technical terms related to the system can be found in [4][5].

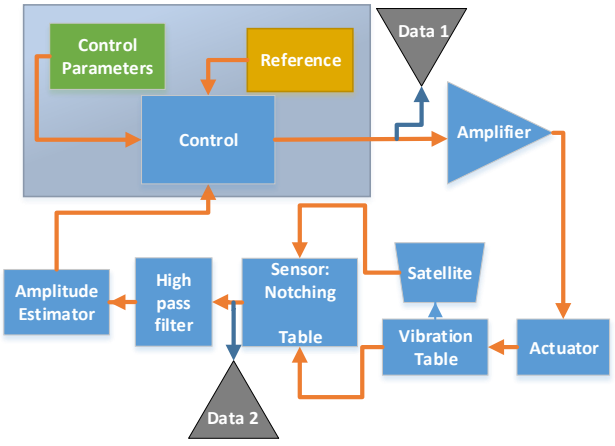

Figure 1 – Current closed-loop system architecture

As shown in Fig. 1, the reference signal and the control parameters are predefined at the beginning of the test. The current control methods [2] generate the acceleration command to the amplifier, which converts the acceleration to necessary force for the actuator. The actuator is linked to the vibration table to transmit the vibration to the satellite. The control accelerometers measure the acceleration of the table, whether the notch accelerometers are placed in the satellite structure and measure the satellites acceleration. A high pass filter with a corner frequency of 0.5 Hz eliminates the DC component of the signal. The filtered value of the measurement signal is then used to estimate the maximum amplitude of each pseudo period, which is compared with the reference amplitude to deduce error and necessary control effort [2][5]. For an experimental test, the control input (data 1 in Fig. 1) and the output (data 2 in Fig. 1) signals are used to determine an input-output model of the composite plant.

Since the paper mainly focuses on the controller design, the elaboration of the 7th order discrete time model through an appropriate estimation procedure based on [5][17] is not detailed here. This estimated model represents the first two modes of the satellite in the range 5 to 50 Hz. In this work, a continuous time modeling of the plant and of the controller is preferred since it is easier to compare to the real plant. Thus, the discrete time model is converted into a continuous time one, using a bilinear transformation [18], without losing any significant information in the range of 5 to 50 Hz. In Fig. 2, the magnitude response with respect to frequency of the discrete time and the continuous time models are compared. It can be noticed that the continuous time model only shifts 0.1 Hz to the right in the first mode and 0.2 Hz in the second mode compared to the discrete time model, without any noticeable difference in the magnitude.

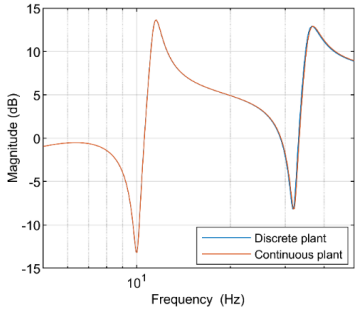

Figure 2 Magnitude response of the full order model

B. Model reduction

In a second step, the obtained continuous time model is reduced in order to decrease the complexity. The order reduction is performed by considering the Hankel's singular values of the full-order model by following a classical approach detailed in the sequel.

First, the Hankel's singular values are ranked considering their multiplicative error bound, which gives the energy of states [19]. The last two states seem to be less significant as they are less than 0.02 compared to other five states, higher than 0.5. They are then removed from the model, leading to a 5th order model.

Then, the model reduction is realized via multiplicative error balanced stochastic model truncation (BST), as it appears to emphasize a specific part of the plant (5 to 50 Hz) [19]. Consequently, within this specific frequency range, the BST method leads to an error lower than the additive reduction. In Fig. 3, it can be noticed that the BST method (blue) gives the best approximation. In the anti-resonance frequencies, an approximate difference with the original plant is kept under 0.2 dB, while in the case of balanced method (red), the error attains approximately 1.9 dB compared to the original plant.

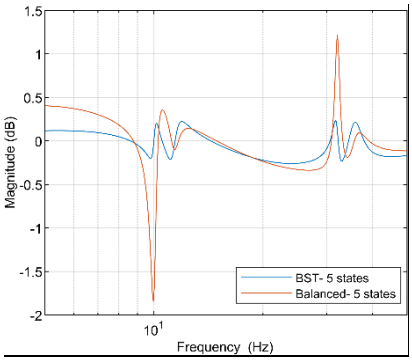

Figure 3 Comparison of error between BST and balanced reduction

C. Modal parameter identification

In the last step of modeling, modal parameters of the plant are determined, obtained from the fifth order model derived above. This model will be used for control design and robustness analysis. The general form of a fifth order transfer function can be written as follows:

$$\frac{B(s)}{A(s)} = \frac{b_5 s^5 + b_4 s^4 + b_3 s^3 + b_2 s^2 + b_1 s + b_0}{s^5 + a_1 s^4 + a_2 s^3 + a_3 s^2 + a_4 s + a_5} \quad (1)$$

where s is the Laplace variable, $a_{1..5}$ and $b_{1..5}$ are the denominator and numerator coefficients respectively. Using the partial fraction decomposition [25] of eq. (1) leads to:

$$\frac{B(s)}{A(s)} = \underbrace{\frac{R_1}{s-P_1} + \frac{R_2}{s-P_2}}_{1} + \underbrace{\frac{R_3}{s-P_3} + \frac{R_4}{s-P_4}}_{2} + \underbrace{\frac{R_5}{s-P_5}}_{3} + R_6 \quad (2)$$

$P_1 .. P_5$ are the poles of the model, $R_1 .. R_5$ the numerator complex coefficients, R_6 a real gain. As the plant contains two modes, consequently, there are two pairs of conjugate poles for each mode and a real 5th pole. In eq. (2), conjugate poles and numerators are gathered, which leads to:

$$\frac{B(s)}{A(s)} = \underbrace{\frac{r_1 - i\,p_1}{s+(m_1 - i\,n_1)} + \frac{r_1 + i\,p_1}{s+(m_1 + i\,n_1)}}_{1} + \underbrace{\frac{r_2 - i\,p_2}{s+(m_2 - i\,n_2)} + \frac{r_2 + i\,p_2}{s+(m_2 + i\,n_2)}}_{2} + \underbrace{\frac{r_3}{s+m_3}}_{3} + R_6 \quad (3)$$

Eq. (3) is a detailed form of eq. (2), where the complex poles and zeros are expressed in terms of real and imaginary parts. Then eq. (3) can be rewritten by redefining variables to obtain modal parameters in view of a parametric design model of the plant, as follows:

$$G(s) = \frac{B(s)}{A(s)} = \frac{2s\,r_1 + 2\,(p_1\,\Omega_1\sqrt{1+\xi_1^2} + r_1\,\Omega_1\,\xi_1)}{s^2 + 2\,\Omega_1\,\xi_1\,s + \Omega_1^2} + \frac{2s\,r_2 + 2\,(p_2\,\Omega_2\sqrt{1+\xi_2^2} + r_2\,\Omega_2\,\xi_2)}{s^2 + 2\,\Omega_2\,\xi_2\,s + \Omega_2^2} + \frac{r_3}{s+m_3} + R_6 \quad (4)$$

Eq. (4) exhibit the modal parameters such as the mode frequency and mode damping, (Ω_1, ξ_1) for the first mode and (Ω_2, ξ_2) for the second mode. They are obtained from Eq. (3):

$$\Omega_1^2 = m_1^2 + n_1^2 \quad - \quad \Omega_2^2 = m_2^2 + n_2^2 \quad - \quad \xi_1 = \frac{m_1^2}{\sqrt{m_1^2 + n_1^2}} \quad - \quad \xi_2 = \frac{m_2^2}{\sqrt{m_2^2 + n_2^2}}$$

III. Proposed Control Architecture

The proposed architecture of Fig. 4 uses an additional feedforward action, which is the inverse of the nominal plant model, to deliver an accurate anticipative command to the actuator. The multivariable two input one output feedback controller is used to compensate tracking error and noise-disturbance. This structure will facilitate the design of the robust controller, leading to an increase of the robustness of the system against modal parameter variations. In general, this strategy increases the bandwidth of the control and the gain of correction, solving the issue of pole-zero compensation of a lightly damped structure [13].

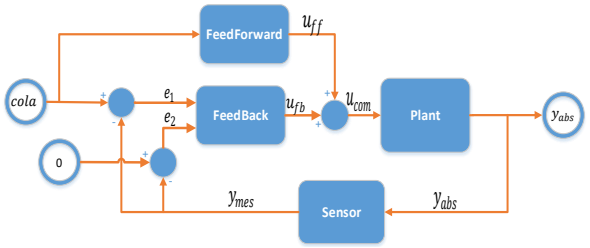

Figure 4 Proposed closed-loop system architecture

The first reference input is a sinusoidal acceleration signal with variable frequency called $cola$ [1][4] and the second one is a constant value of 0 [20], that emphasizes the cancellation of the disturbance action on the output. The errors associated to the references are denoted respectively e_1 and e_2. The control effort, u_{com}, is the sum of the feedforward action, denoted u_{ff}, and the feedback action denoted u_{fb}. y_{abs} and y_{mes} are the real and measured output acceleration.

A. Closed-loop specification

Let first define the specification of the closed-loop system from an industrial point of view. The tracking error has to be kept less than $\pm 1\%$ of the amplitude of $cola$ (can reach upto 2g) under parameter variation, resulting in a significant vibration reduction of the system. Given the actuation limit of 75g, the closed-loop system must use the minimum control effort and keep it below the saturation limit. In this paper, we limit the analysis to a single mode of the satellite, which is between 5 to 20 Hz and we emphasize the performance of the system in terms of modal parameter variations of that given mode. There are mainly two factors, which introduce parameter variations of the system. Firstly, the derivation of the continuous time synthesis model from the full order identified discrete time model accounts for almost 1.5% of uncertainties on the mode damping. Moreover, the dynamics identified from a very low-level test differs from the qualification level test by a frequency shift of -5% and 15% of damping. Lastly, an analysis is required to ensure the stability of the system.

B. H_∞ feedback control synthesis

Firstly, the industrial specifications are transformed into frequency domain constraints in order to derive an optimization problem formulation [2][21]. Fig. 5 defines the closed-loop synthesis model.

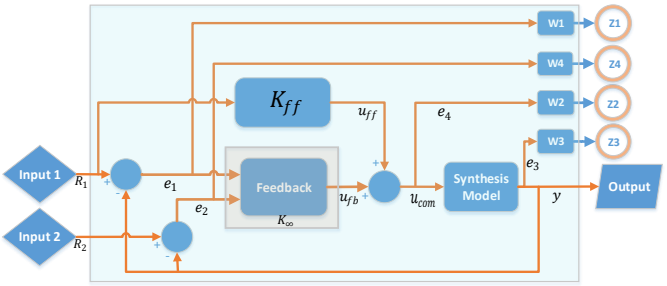

Figure 5 H_∞ synthesis architecture

The frequency domain constraints are imposed on the system via four weighting functions, denoted w_1, w_2, w_3 and w_4.

The feedforward controller $K_{ff}(s)$ is defined by:

$$K_{ff}(s) = G_{nom}(s)^{-1} \tag{5}$$

where $G_{nom}(s)$ is the plant dynamics obtained from eq. (4) with the nominal values of (Ω_1, ξ_1) and (Ω_2, ξ_2).

1) Problem formulation

The controller $K_\infty(s)$ has to satisfy performance criteria defined by frequency domain weights. Fig. (6) illustrates the linear fractional transformation (LFT) of the given problem.

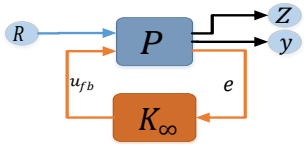

Figure 6 LFT model

In Fig. 6, $R = [R_1\ R_2]^T = [cola\ 0]^T$ is the reference input, $e = [e_1\ e_2]^T$ the tracking error and $Z = [z_1\ z_2\ z_3\ z_4]^T$ the exogenous output. The LFT associated to Fig. 6 can be written as:

$$\begin{bmatrix} Z \\ y \\ e \end{bmatrix} = P(s) \begin{bmatrix} R \\ u_{fb} \end{bmatrix} \tag{6}$$

The expression of $P(s)$ is given below:

$$P(s) = \begin{bmatrix} w_1 - w_1 G K_{ff} & 0 & -w_1 G \\ w_2 K_{ff} & 0 & w_2 \\ w_3 G K_{ff} & 0 & w_3 G \\ -w_4 G K_{ff} & w_4 & -w_4 G \\ -G K_{ff} & 0 & G \\ I - G K_{ff} & 0 & -G \\ -G K_{ff} & I & -G \end{bmatrix} \tag{7}$$

P is the augmented model of Fig. (5) and K_∞ is the feedback controller, then the LFT between P and K_∞ is denoted by $F(P, K_\infty)$.

The definitions of the sensitivity functions are given by:

- Sensitivity: S between e_1 and R_1, we restrain this function to minimize the tracking error of the input $cola$.
- Complementary sensitivity: T between e_3 and R_1 $(cola)$, is used to constrain the effect of sensor noise
- KS between e_4 and $R_1(cola)$ is used to limit the actuator signal

By the application of the small gain theorem [20], we can obtain the design criteria, as follows:

$$\begin{cases} \bar{\sigma}(S(s)\,w_1(s)) & < \gamma \\ \bar{\sigma}(K_\infty\,S(s)\,w_2(s)) & < \gamma \\ \bar{\sigma}(T(s)\,w_3(s)) & < \gamma \end{cases} \tag{8}$$

where $\bar{\sigma}$ is the upper singular value and $\gamma > 0$. The H_∞ feedback controller is obtained by minimizing $\|F(P, K_\infty)\|_\infty$ for the set of $K_\infty(s)$ which stabilizes the internal states of the system. The minimum gain is called H_∞ optimal gain γ_{opt}. From eq. (8) it comes:

$$\|F(P, K_\infty)\|_\infty = \left\| \begin{matrix} S(s)\,w_1(s) \\ K_\infty\,S(s)\,w_2(s) \\ T(s)\,w_3(s) \end{matrix} \right\|_\infty < \gamma_{opt} \tag{9}$$

C. Weight selection for H_∞ control

In this section, we introduce a systematic way to transform the industrial specifications of the closed loop vibration testing system to frequency domain weights w_1, w_2 and w_3. The tracking error is constrained via the weight $\frac{1}{w_1}$ [21]. As previously mentioned, considering the dynamic tracking, time domain verification is needed to quantify the tracking error of the closed-loop system. As we intend to evaluate up to 20 Hz including the first mode, w_1 is chosen to constrain the magnitude near 20 Hz at approximately -20 dB and the bandwidth of this weight is 147 Hz. This value is chosen as small as possible, since a higher corner frequency of $\frac{1}{w_1}$ will result in a controller with bad noise filtering properties at lower frequencies. The chosen weighting function is:

$$\frac{1}{w_1} = \frac{1.4\,s + 0.14}{s + 1571} \tag{10}$$

The specification is to limit the bandwidth of the complementary sensitivity function as low as possible to filter as much as possible sensor noises. At the same time, we cannot lower this value arbitrarily as we need a minimum bandwidth to keep the tracking error within the tolerance. So the bandwidth of this weight has been fixed at a minimum value, which is 443 Hz, and its magnitude crosses 0 dB at 254 Hz to satisfy the H_∞ optimization criteria.

$$\frac{1}{w_3} = \frac{2287\,s + 2.615\,10^8}{1.144\,10^5\,s + 1.868\,10^8} \tag{11}$$

The low frequency amplitude has been set at the maximum value of acceleration (75 g) delivered by the vibrator. It reaches 0 dB at the maximum operative frequency (1700 Hz) of the vibrator. The expression of $\frac{1}{w_2}$ is given by:

$$\frac{1}{w_2} = \frac{1.037\,10^4\,s + 1.075\,10^9}{1.037\,10^5\,s + 1.433\,10^7} \tag{12}$$

w_4 is further chosen equal to 1, see section IV.A.2. The H_∞ controller is determined for these weighting functions by

solving an optimization problem, using the robust control toolbox of MATLAB [24].

IV. Simulation Results

A. Frequency domain analysis

1) Analysis of the synthesized controller

The designed controller satisfying the constraints of eq. (9) is illustrated in Fig. 7.

As the order of this synthetized controller is the sum of the orders of the different dynamics, (5^{th} order for each of plant and feedforward controller, a single order for each of the three weights), totaling a 13^{th} order controller, which remains acceptable in the real time simulation using a typical intel 3^{rd} generation dual core I3 processor clocked at 3.2 GHz.

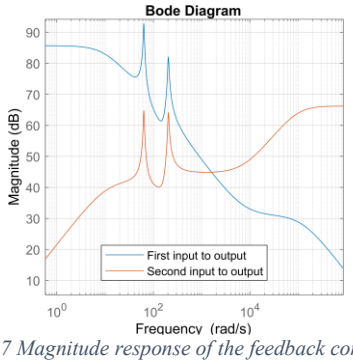

Figure 7 Magnitude response of the feedback controller

2) Analysis of the sensitivity functions

The optimization problem leads to $\gamma_{opt} = 0.98$. Before any further analysis, it is important to mention that the second input of the controller of Fig. 4, with the weight w_4, is used to satisfy the optimization criterion, as only one single input resulted in a very high γ_{opt} (almost 50), leading to a non-respect of the specifications. Fig. 8 shows the sensitivity functions, remaining below their corresponding weights of eq. (9), satisfying the frequency domain specifications.

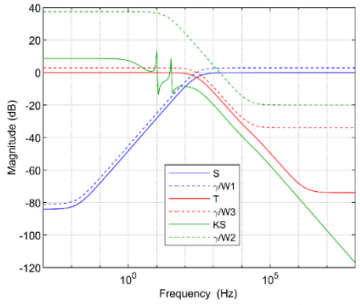

Figure 8 Constraints vs sensitivity functions

3) Stability margin

The open-loop two-input two-output function is given by:

$$T_{OL} = G\,K_{\infty} \tag{13}$$

The closed-loop transfer of this open-loop system is expressed by:

$$T_{CL} = \left(I + T_{OL}\right)^{-1} \tag{14}$$

By using the unstructured small gain theorem, the guaranteed minimum margin of the two loop is given by α_{max} [20]:

$$\alpha_{\max} = \frac{1}{\sup_{w} \bar{\sigma}(T_{CL}^{-1})} \tag{15}$$

The guaranteed margin is $\alpha_{max} = 0.71$, which can be used to deduce the stability margin through the following relations:

$$\begin{cases} \dfrac{1}{1+\alpha_{\max}} < GM < \dfrac{1}{1+\alpha_{\max}} \\ |\varphi_i| < 2\sin^{-1}\left(\dfrac{\alpha_{\max}}{2}\right) \end{cases} \tag{16}$$

where GM denotes the gain margin and φ_i is for phase margin, which are respectively (0.6, 3.41) and $\pm 41.4°$. The obtained stability margins indicate that the system dynamics can vary up to the upper and lower limits of gain and phase margins before being unstable.

B. Time domain analysis

Time domain analysis has been achieved using the system described in Fig. 4.

1) Nominal case study

In this part, the dynamics of the system is calculated from eq. (4) with nominal modal parameter values, the analysis has been done in the frequency range of $[5, 20]$ Hz, for a sweep rate of 3 oct/min.

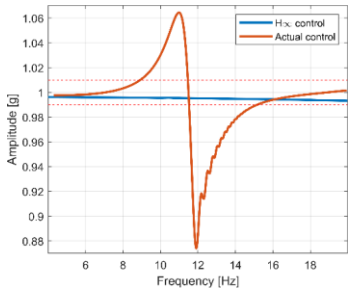

Figure 9 Tracking performance of a nominal plant dynamics

For this given study case, the result of Fig. 9 shows that the dynamic tracking error between the reference and the measured acceleration amplitude (H_{∞} control, blue) is below $\pm 1\%$. At the same time, the performance of the current nonlinear controller [2] for the same case (in red) shows a degraded performance (max. error reaches [-13%, 5%]).

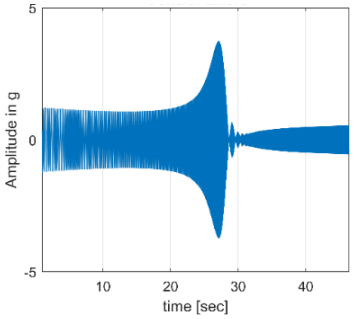

Figure 10 Total control effort u_{com}

Fig. 10 illustrates the total control effort u_{com}, which is the sum of the feedforward and feedback actions. We find that the maximum amplitude near 27 sec reaches roughly ± 3.73 g, when capacity is 75g. It can also be remarked that the correction in lower frequencies needs higher actuation.

2) Robustness study

In this section, we intend to demonstrate the robust performance of the proposed H_∞ controller against modal parameter (Ω_1, ξ_1) variation. Fig. (11) shows the magnitude response of the set of plants with $\pm 15\%$ of the mode frequency (Ω_1) variations and $\pm 25\%$ of the damping (ξ_1) variations. Those parameters are distributed to their limits in order to create the worst-case scenarios, which therefore validates the range of obtainable dispersion through the proposed control architecture.

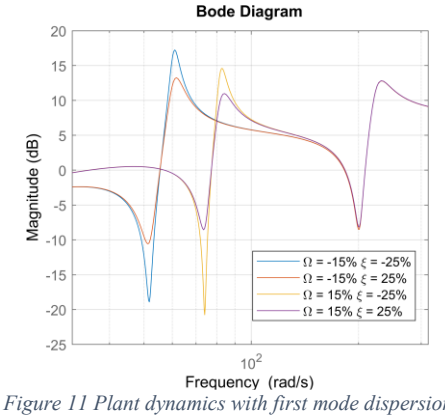

Figure 11 Plant dynamics with first mode dispersion

The error amplitude in Fig. 12 evidences the robustness against $\pm 15\%$ of frequency (Ω_1) shift (3 times more than the required specification) and $\pm 25\%$ of damping (ξ_1) (almost $\pm 8\%$ more than the specification). The tracking error is kept below $\pm 1\%$ without any further vibrations.

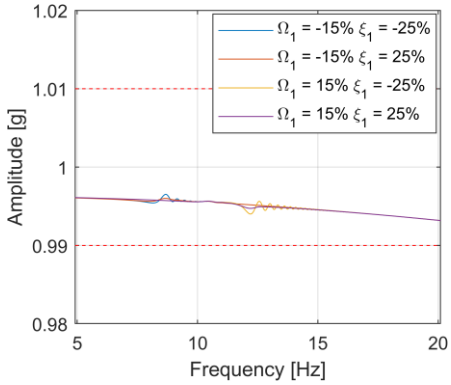

Figure 12 Robust performance of the H_∞ controller

The combination of right frequency shift and lightest damping factor appears as the worst case, and pushing those limits higher induces oscillations near 1g.

V. Conclusion

The main goal of the paper is to propose a control architecture of the vibration testing system, which limits dynamic tracking error in presence of modal parameter variation, while optimizing the control effort to stay below the actuator saturation. The proposed feedforward-feedback control system also gives an alternative for pole/zero cancellation issues of classical H_∞ mixed sensitivity problems observed in the active vibration control systems. The control structure is kept to a minimal order of complexity, making it implementable for the vibration testing system of lightly damped large space structures. Ongoing work considers the study of several modes and as a perspective, the experimental validation of the controller.

References

[1] "Spacecraft mechanical loads analysis handbook," European Cooperation for Space Standardization, February 2013.

[2] S. Arefin, D. Dumur, A. Bettachioli, A. Hot, and S. Tebbani, "Sine sweep tracking control of lightly-damped spacecraft," ICSTCC, 2020.

[3] A. Bettacchioli, "Feasibility study of the beating cancellation during the satellite vibration test," ECSSMET, Toulouse, September 2016.

[4] A. Bettacchioli, P. Nali, "Common issues in S/C sine vibration testing," 29th Aerospace Seminar, Los Angeles, October 2015.

[5] A. Bettacchioli, "Simulation of satellite vibration test," ECSSMET, Braunschweig, April, 2014

[6] I. Liu and X. Wang, "Advanced Sliding Mode Control for Mechanical Systems," Tsinghua University Press, Beijing, 2011.

[7] B. Bandyyopadhyay, S. Janardhan, and S. K. Spurgeon, "Advances in Sliding Mode Control," Springer-Verlag Berlin Heidelberg 2013.

[8] A. Bettacchioli, P. Nali, "Beating Phenomena in spacecraft sine test," ECSSMET, Braunschweig, April, 2014

[9] "Ariane 5 User's Manual" Arianespace. Issue 5 – Rev. 1, July 2011.

[10] A. Preumont, "Vibration control of active structures: an introduction". Vol. 246. Springer, 2018.

[11] W. Gawronski, "Advanced Structural Dynamics and Active Control of Structures". Springer-Verlag New York, 2004.

[12] G. Balas, "Robust control of flexible structures: theory and experiments", Doctoral dissertation Caltec, 1990.

[13] P. Gahinet, and P. Apkarian, "A Linear Matrix Inequality Approach to H_∞ Control," Int. J. Robust and Nonlinear Contr., vol. 4, 1994.

[14] M. C. Tsai, E. J. M. Geddes and I. Postlethwaite, "Pole-zero cancellations and closed-loop properties of an H_∞ mixed sensitivity design problem," Automatica, Volume 28, Issue 3, May 1992.

[15] A. Mystkowski, "An application of mu-synthesis for control of a small air vehicle," Journal of Vibroengineering 14(1):79-86, March 2012.

[16] C. Naisse and A. Bettacchioli, "Simulation des essais en vibrations de satellites a partir de l'analyse modale dune reponse bas niveau," A.S.T.E. n111, 2012.

[17] D. W. Clarke, "Generalized least squares estimation of the parameters of a dynamic model," IFAC Symp. on Identification in Autom. Cont. Systems, Prague, 1967, paper 3.

[18] K. J. Astrom, "Computer Controlled Systems, Theory and Design," Second ed., 1990. Prentice-Hall. p. 212. ISBN 0-13-168600-3.

[19] M.G. Safonov, and R.Y. Chiang, "Model Reduction for Robust Control: A Schur Relative Error Method," International J. of Adaptive Control and Signal Processing, Vol. 2, pp. 259-272, 1988.

[20] K. Zhou, J.C. Doyle, K. Glover, "Robust and Optimal Control," Prentice-Hall, 1996.

[21] D.W. Gu, P. Petkov, and M. M. Konstantinov, "Robust control design with MATLAB®", Springer Science & Business Media, 2005.

[22] K. Gernaey, J. Huusom and R. Gani, "12th International Symposium on Process Systems Engineering," Vol. 37, 1st Edition, Elsevier, 2015.

[23] R. Vilanova, "Reference controller design in 2-DOF control," Electr Eng 90, 275–281 (2008).

[24] Glover, K., and J.C. Doyle. "State-space formulae for all stabilizing controllers that satisfy an H_∞ norm bound and relations to risk sensitivity." Systems & Control Letters, Vol. 11, Number 8, 1988, pp. 167‑172.

[25] K. R. Rao and N. Ahmed, "Recursive techniques for obtaining the partial fraction expansion of a rational function," IEEE Trans. Educ. 11, 1968. pp. 152–154. doi:10.1109/TE.1968.43203